Journal of Inorganic and Organometallic Polymers and Materials
https://doi.org/10.1007/s10904-019-01098-z

# Nano-synthesis, Biological Efficiency and DNA Binding Affinity of New Homo-binuclear Metal Complexes with Sulfa Azo Dye Based Ligand for Further Pharmaceutical Applications

**Fawaz A. Saad[1] · Hoda A. El-Ghamry[1,2] · Mohammed A. Kassem[1,3] · Abdalla M. Khedr[1,2]**

Received: 24 December 2018 / Accepted: 4 February 2019


**Abstract**
Five novel nanometric homo-binuclear complexes have been synthesized by the reaction of Cu(II), Co(II), Ni(II), Mn(II) and Zn(II) salts with a new azo dye 4-(2,4-dihydroxy-phenylazo)-*N*-thiazol-2-yl-benzenesulfonamide ($H_2L$) with the aim to develop neoteric antitumor drugs. $H_2L$ has been prepared by coupling of sulfathiazole with resorcinol in order to comprise the bioactivities of sulfonamide part and azo group in the formed metal complexes which greatly enhance their bio-efficiencies. The ligand and complexes have been fully characterized using various spectral and analytical techniques. The obtained data indicated a dibasic tetradentate nature of ligand which coordinated via deprotonated phenolic oxygen, one azo group nitrogen, N-atom of thiazole ring, and sulfonamide oxygen forming tetrahedral geometry around the central metal ions. XRD data confirmed the crystalline nature of ligand and amorphous nature of the complexes. TEM images proved nanometeric size of complexes particles. The data of antimicrobial screening revealed that metal complexes are more potent than the azo dye ligand against varies micro-organisms. Anticancer activities of all compounds were evaluated against human liver carcinoma cells (HepG-2) and breast carcinoma cells (MCF-7). Cu(II) complex showed the highest anticancer activity ($IC_{50}$ = 23.6 µg/ml) against HepG-2 cells. Co(II) complex displayed the greatest anticancer activity ($IC_{50}$ of 7.67 µg/ml) contra MCF-7 cells. Electronic absorption and viscosity studies proved that $H_2L$ and complexes interact with DNA by intercalation binding and electrostatic force groove binding modes, respectively. The results of this study ascertain that Cu(II) and Co(II) complexes are very favorable candidates for further applications in cancer therapy.

**Keywords** Nano-meter complexes · Sulfathiazole · Characterization · Anticancer · DNA binding

## 1 Introduction

Sulfa compounds are well known as useful antibiotics in the assorted microbial contagion treatment [1–3]. Nevertheless, the high applications of these compounds stimulate allergic side effects to many body organs [4, 5] as well as lymphadenopathy, hepatotoxicity, and haematological disorders [6]. In order to beat such quandaries and to make efficient drugs, new functionalized sulfonamide derivatives and their transition metal complexes [7–10] were in clinical trials. Metal sulfonamide complexes were more effective than the drugs, which they come from [11]. Also, the azo dyes have been testified to display diversity in bio-vitality, involving anti-inflammatory [12], antibacterial [13], and antiviral [14] activities. Among these azo dye compounds, sulfathiazole azo dyes and their metal complexes have gained considerable attention due to their bio-efficiency in different biological and therapeutic applications [15–18]. Furthermore, bi and poly-nuclear metal complexes have been attracted increasing attention as a result of their fabulous uses in biological systems [19], and gorgeous applications in the field of material sciences [20], beside their marvelous spectroscopic and magnetic characteristics [21]. On the other side, the

**Electronic supplementary material** The online version of this article (https://doi.org/10.1007/s10904-019-01098-z) contains supplementary material, which is available to authorized users.

✉ Hoda A. El-Ghamry
helghamrymo@yahoo.com

[1] Department of Chemistry, Faculty of Applied Science, Umm Al-Qura University, Makkah, Saudi Arabia

[2] Chemistry Department, Faculty of Science, Tanta University, Tanta, Egypt

[3] Chemistry Department, Faculty of Science, Benha University, Benha, Egypt

Published online: 11 February 2019

interaction between DNA and small molecules is a favorable field of scientific research as it is as an overlapped area between biology and chemistry [22]. Such small molecules connect with DNA through weak forces such as π-stacking reactions, which often escorted with inter pupation of the aromatic (planar) constituent between base pairs of the different types of deoxyribonucleic acid, in addition to the weak physical interactions of functionalities group through the groove of the DNA [23]. A great number of research works are directed to the designing of conformation- and site- specified reagents provide rationales for unprecedented drug styling as well as improve susceptible chemical probes for the structure of DNA. In the recent few years, the interactions between metal complexes and nucleic acids and have profited great interest due to their importance in the evolution of novel reagents for biotechnology and medicament [24]. In the present paper, we had accomplished coupling of sulfathiazolyl-diazonium salt and resorcinol, in order to prepare 4-(2,4-dihydroxy-phenylazo)-*N*-thiazol-2-yl-benzenesulfonamide ($H_2L$), which were applied to synthesize nano-sized divalent Cu, Co, Ni, Mn and Zn complexes. The structures of all complexes were elucidated using elemental and thermal (TG) analyses, spectrophotometric, ESR, FT-IR, XRD, TEM, and magnetic measurements. The interaction of $H_2L$ and its complexes with DNA were followed by electronic absorption titration and viscosity methods, keeping in mind, the dignified importance of inspecting the interaction of nucleic acids with metal complexes in developing novel reagents for biotechnological and medicinal uses. In-vitro examinations for antimicrobial and antitumor efficiencies were performed for all investigated compounds to test their potency therapeutic efficiencies as new curative agents.

## 2 Experimental

### 2.1 Synthesis of Sulfa Thiazolyl-Azo-Resorcinol ($H_2L$) Ligand

The azo dye 4-(2,4-dihydroxy-phenylazo)-N-thiazol-2-yl-benzenesulfonamide ($H_2L$) were prepared by the following recommended procedures. A suspension solution of 4-amino-N-(1,3-thiazol-2-yl)benzenesulfonamide (2.55 g, 0.001 mol) in diluted HCl (15.0 ml HCl + 15.0 ml $H_2O$) was heated to 75 °C till formation of clear solution. The obtained aqueous solution was cooled bellow 5 °C and diazotized using $NaNO_2$ (1.5 g dissolved in 15 ml $H_2O$). To resorcinol solution, (1.10 g, 0.001 mol) in $H_2O$ containing NaOH (1.6 g), the formed diazonium salt was added drop-wise through the course of 30 min at 0 °C, with contentious stirring. The acquired formed precipitate was filtrated off using whatman filter paper and washed three times at least. The obtained sulfa thiazolyl-azo-resorcinol ligand, $H_2L$ (Fig. 1) was re-crystallized many times.

### 2.2 Nano-synthesis of Metal Complexes with Sulfa Thiazolyl-Azo-Resorcinol Ligand

The well-known reflux-precipitation technique was applied in order to synthesize the nano-sized transition metal complexes as the following. To a flask containing sulfa thiazolyl-azo-resorcinol ligand, $H_2L$ (0.001 mol in 40 ml of $C_2H_5OH$), the different divalent metal salts solutions (0.001 and/or 0.002 mol dissolved in 30 ml 50% (V/V) $H_2O$–$C_2H_5OH$ mixture were added, drop by drop with continuous stirring. The formed mixtures were allowed to reflux for about 10–15 h, and then, allowed to cool, and the ethanol was evaporated under reduced pressure. The precipitated metal complexes formed (after addition of few drops of triethylamine), were collected by filteration and washed with ethanol then diethylether. The obtained solids were dried out using a dissector over anhydrous $CaCl_2$. The purities of gained metal complexes were examined applying thin layer chromatography (TLC).

### 2.3 Methods, Physical and Analytical Measurements

Carbon, hydrogen and nitrogen contents for the prepared compounds were achieved using a 2400 CHN Elemental Analyzer (Perkin–Elmer). Sherwood magnetic susceptibility balance was used to determine the room temperature magnetic moment values of complexes **1**–**5**. Applying Nujol mull technique, electronic absorption spectra of all compounds were measured by the aid of a Shimadzu spectrometer (model UV-3600). In a DMF solvent ($10^{-3}$ mol $l^{-1}$), the molar conductance was performed using a JENWAY (model 4070) conductance bridge. FT-IR measurements of all inspected compounds were measured by FT-IR Bruker Tensor 27 spectrophotometer within a range of 4000–200 $cm^{-1}$, as KBr disks. ESR spectrum (X-band) of powder Cu(II) complex was achieved using a Jeol JES-RE1X EPR spectrometer (υ = 9.435 GHz, at Alexandria University). A Shimadzu TG-50 thermal analyzer was used in

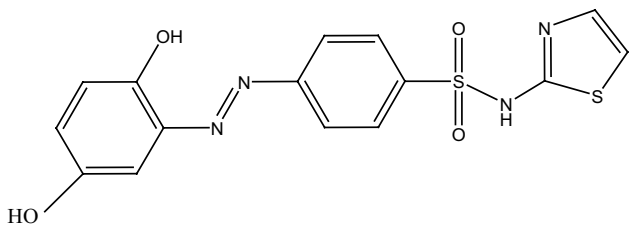


**Fig. 1** Molecular structure of the sulfathiazolyl-azo-resorcinol ligand, $H_2L$

order to investigate the thermo-gravimetric analysis (TGA) of complexes **1**–**5**, using 10 °C/min heating rate, in presence of $N_2$ as atmosphere. XRD patterns for the examined compounds were recorded using GNR X-ray diffractometer (APD2000PRO) in presence of Cu/K$\alpha_1$ radiation applying a graphite monochromator (at 0.03° $min^{-1}$ scanning rate). The in-vitro antitumor activity of all inspected compounds was examined contra *Hepatocellular* carcinoma cell lines (HepG-2) compared with cis-DDP as standard agent and *Breast* carcinoma cell lines (MCF-7) compared with 5-flurouracil as standard agent, applying the well-known recommended techniques [25, 26]. The antimicrobial resistance of $H_2L$ and metal chelates under investigation was estimated against *Aspergillus fumigatus* (RCMB 002008), *Candida albicans* RCMB 005003 (1) ATCC 10,231, *Staphylococcus aureus* (RCMB010010) and *Salmonella typhimurium* RCMB 006 (1) ATCC 14,028, applying diffusion agar method [27].

### 2.4 Methods of DNA Binding Mode Investigation

The manner of binding between salmon serum DNA (SS DNA), the inspected ligand and its chelates were investigated by two techniques [28], due to the tremendous importance of investigating the type of association among small compounds and deoxyribonucleic acid in the improvement of novel curative reagents for medicine and biotechnology. The first applied technique is the electronic absorption spectroscopic titration where we increased the amounts of DNA solution added to a specified concentration of the tested compound and measured the electronic spectra for different solutions. The $K_b$ (authentic binding constant) values were calculated from the obtained data. Using the obtained binding constant values, we can determine whether the binding mode between the tested compounds and DNA is intercalative or non-intercalative [28]. The second technique depends on the viscosity studies, which shows comprehensive precision to any alteration in the length of DNA. In this technique, DNA specific viscosity was estimated using various concentrations of the tested compound while the concentration of DNA was kept fixed. The gained results were plotted as $(\eta/\eta_0)^{1/3}$ against [compound]/[DNA] (mole ratio), where η is the viscosity of DNA in the presence of inspected compound and $\eta_0$ is the viscosity of DNA without the tested compound. The using of viscosity technique is considered conventional one that is usually applied in order to estimate the DNA binding mode in solutions.

## 3 Results and Discussion

### 3.1 Elemental Analysis and Conductance Measurements

The secured results obtained from elemental m*icro-analysis* of the free organic sulfathiazolyl-azo-resorcinol ligand, $H_2L$ and complexes **1**–**5** are extremely agree with the proposed molecular formulae. The information presented in Table 1 assert formation of 2:1 (M:L) stoichiometry for all complexes. The values of molar conductance determined for complexes **1**–**5**, in a concentration of $1 \times 10^{-3}$ M solution dissolved in DMF, were found to be within 13.4–27.6 $\Omega^{-1}$ $cm^2$ $mol^{-1}$ range, revealing the non-electrolytic nature of all chelates [29].

### 3.2 IR Spectra and Binding Mode

For investigating the coordination sits in sulfathiazolyl-azo-resorcinol ligand, $H_2L$ that participate in bond formation with the metallic centers, the FT-IR spectra of complexes **1**–**5** are inspected and compared with that of the free ligand (Fig. 1S). The essential peaks in $H_2L$ spectrum are applied to direct us to grasp this affair. Upon complex formation,

**Table 1** Micro-analysis and physical characteristic of sulfa thiazolyl-azo dye ligand and complexes **1**–**5**

| Comp. no. | Molecular formula (empirical formulae) | Color (mol. wt.) | m. p. (yield) | Microanalysis, calc. (found) % | | |
|---|---|---|---|---|---|---|
| | | | | C% | H% | N% |
| $H_2L$ | $C_{15}H_{12}N_4O_4S_2$ | Orange (376.03) | 182 (89) | 47.86 (47.93) | 3.21 (3.25) | 14.88 (14.91) |
| **1** | $[LCu_2Cl_2(H_2O)_2]\cdot 2H_2O$ $C_{15}H_{18}Cl_2Cu_2N_4O_8S_2$ | Brown (644.45) | > 300 (71) | 27.96 (28.03) | 2.82 (2.76) | 8.69 (8.74) |
| **2** | $[LCo_2Cl_2(H_2O)_2]\cdot 2H_2O$ $C_{15}H_{18}Cl_2Co_2N_4O_8S_2$ | Dark brown (635.23) | > 300 (65) | 28.36 (28.44) | 2.86 (2.95) | 8.82 (9.03) |
| **3** | $[LNi_2Cl_2(MeOH)_2]$ $C_{17}H_{18}Cl_2N_4Ni_2O_6S_2$ | Red (626.77) | > 300 (82) | 32.58 (32.07) | 2.89 (3.12) | 8.94 (9.17) |
| **4** | $[LMn_2Cl_2(H_2O)_2]$ $C_{15}H_{14}Cl_2Mn_2N_4O_6S_2$ | Deep red (591.21) | > 300 (61) | 30.47 (30.53) | 2.39 (2.43) | 9.48 (9.70) |
| **5** | $[LZn_2(SO_4)_2]\cdot 2H_2O$ $C_{15}H_{16}N_4O_{14}S_4Zn_2$ | Red (735.35) | > 300 (77) | 24.50 (24.50) | 2.19 (2.25) | 7.62 (7.58) |

these peaks often show alterations either in their shapes, positions, and/or their intensities while some of them vanish upon chelation. The IR spectral bands of intrinsic significance for sulfathiazolyl-azo-resorcinol ligand, $H_2L$ and metal chelates **1**–**5**, are presented in Table 2. $H_2L$ spectrum showed a broad band at 3450 $cm^{-1}$, this band assigned to the stretching vibrations of intra-molecular hydrogen bonded hydroxyl group [30], and a band appeared at 3228 $cm^{-1}$ is attributed to $\nu_{NH}$. Complexes **1**–**5** displayed broad bands within 3413–3426 $cm^{-1}$ range assigned to $\nu_{OH}$ of solvent molecules binding with the studied chelates. Furthermore, these chelates showed feeble bands at 781–806 $cm^{-1}$ range corresponding to $\delta(H_2O)$ of coordinated molecules [31]. The band manifested in the ligand spectrum at 1478 $cm^{-1}$ is specified to $\nu_{N=N}$. These bands displayed observable shifts to higher wavenumbers by 17–35 $cm^{-1}$ upon complex formation asserting its chelation toward metallic centers through the azo nitrogen atom. The ligand band observed at 1245 $cm^{-1}$ was attributed to $\nu_{C-O}$ bond. This band underwent obvious variation in the metal chelate spectra supporting the interaction of the α-position hydroxyl group in complex formation through proton displacement; except for complex **5**, in which the hydroxyl group attached to the metallic sit. The band detected for the considered ligand at 1621 $cm^{-1}$ was attributed to $\nu_{C=N}$ bond of thiazole ring. The observed shift in this band for all prepared chelates, is assigned to its participation in the complex formation. The non-ligand bands appearing within the ranges 467−434 and 574−525 $cm^{-1}$ for chelates were attributed to M–N and M–O stretching vibrations, respectively [32].

### 3.3 Thermal Gravimetric Analytical Studies

Thermo-gravimetric analytical information is an essential source in concluding the molecular structure of the metal complexes [33, 34], which providing valuable data about their thermal degradation stages, nature of intermediate, thermal features, and the residual products of their thermal decompositions [35]. It has significant importance in recognizing the types and percent's $H_2O$ and/or organic solvent molecules as well as the anionic groups attached to the metallic centers. The thermal gravimetric analyses (TGA) of the inspected solid complexes **1–5** were investigated. The essential thermal decomposition steps, intermediates properties, decomposition temperature ranges, and definitive degradation, in addition to the found and theoretical calculated weight loss percent in each decomposition stage are presented in Table 1S and the TG thermograms are displayed in Fig. 2S. It is obvious from the TG thermograms that the complexes, **1–5**, decomposes through three (complex **2**), four (complexes **1, 4** and **5**) or five successive decomposition steps (complex **3**). Analysis of the weight loss during the first step is consistent with the loss of lattice (complex **5**), coordinated (complexes **3** and **4**) or both lattice and coordinated solvent molecules (complexes **1** and **2**); water or methanol molecules. The coordinated anions (chloride or sulfate) associated with the fractional degradation of the organic part are lost within the second step of decomposition. Complete decomposition of the organic ligands occurs within the third, fourth and fifth step of decomposition involves the formulation of the thermally stable metallic oxide or only metal as residual stable products. The thermal decomposition of compound **4**, as illustrative example, can be illustrated by the following schemes:

$$\left[LMn_2Cl_2\left(H_2O\right)_2\right] \xrightarrow[-5.6\,(calcd.\,6.08\%)]{25-120\,^{\circ}C} \left[LMn_2Cl_2\right]$$

$$\left[LMn_2Cl_2\right] \xrightarrow[-28.73\,(calcd.\,28.94\%)]{120-408\,^{\circ}C} \left[LMn_2\right]$$

$$\left[LMn_2\right] \xrightarrow[-47.17\,(calcd.\,46.21\%)]{408-798\,^{\circ}C} 2Mn$$

These TGA outcomes for the complexes **1–5** substantially supported their proposed molecular composition, as displayed formerly and as shown in Table 1S.

### 3.4 UV–Vis Measurement and Magnetic Moment Studies

Electronic absorption (UV/Vis) measurement is considered one of the most essential tools in differentiation between the various geometrical structures; octahedral, square planar, and tetrahedral of various metal complexes. Also, it plays a useful role in assuring the coordination of ligand constituent atoms with the metal ions. Electronic absorption spectra of sulfathiazolyl-azo-resorcinol ligand, $H_2L$ and its chelates

**Table 2** Assignments for diagnostic important bands in IR spectra for $H_2L$ and complexes **1–5**

| Comp. | ν(OH) | ν(NH) | ν(C=N) | ν(N=N) | ν(C–O) | ν(M–O) | ν(M–N) |
|---|---|---|---|---|---|---|---|
| $H_2L$ | 3450 | 3228 | 1621 | 1478 | 1245 | – | – |
| **1** | 3426 | – | 1604 | 1461 | 1271 | 569 | 434 |
| **2** | 3413 | – | 1594 | 1449 | 1264 | 574 | 467 |
| **3** | 3417 | – | 1592 | 1449 | 1261 | 525 | 448 |
| **4** | 3419 | – | 1610 | 1443 | 1265 | 562 | 439 |
| **5** | 3414 | 3236 | 1596 | 1453 | 1286 | 570 | 443 |

**1–5** were achieved within 200–800 $cm^{-1}$ range applying the Nujol mull technique. The spectrum of $H_2L$-Cu(II), complex **1**, showed a broad peak at 636 nm which attributed to $^2B_{1g} \rightarrow {}^2A_{1g}$ transition, propping a square-planar geometrical configuration around the Cu(II) ion. The peak presented at 366 nm, imputed to $n \rightarrow \pi^*$ transition within the ligand moiety, whereas band appeared 486 nm is corresponding to LMCT [36]. Magnetic moment of $H_2L$-Cu(II), complex **1**, was determined and found to be 1.75 BM. This value is nigh the range of the spin-allowed values expected for one unpaired electron (1.72 BM), upholding the gained electronic spectral results [37]. In case of Co(II) complex **2**, two bands were predestined at the visible region at 507 & 733 nm, which are imputed to $^4A_2 \rightarrow {}^4T_1$ ($\upsilon_2$) and $^4A_2 \rightarrow {}^4T_1(P)$ ($\upsilon_3$) transitions, respectively, supporting four coordinate tetrahedral stereochemistry around Co(II) ions [38]. Also, magnetic moment value of $H_2L$-Co(II), complex **2**, equals 4.26 BM, which is greater than theoretic spin only value for Co(II) complexes revealing the orbital participation of Co(II) complexes [39]. For Ni(II) complex **3**, its electronic spectrum showed three absorption bands at 478, 548 & 752 nm attributed to $^3T_1(F) \rightarrow {}^3T_1(P)$, $^3T_1(F) \rightarrow {}^3A_2(F)$ & $^3T_1(F) \rightarrow {}^3T_2(F)$ transitions that are consistent with Ni(II) tetrahedral complex. The value of counted magnetic moment counted of Ni(II) complexes **3** was 3.43 BM in high consistence with the tetrahedral arrangement of complex [40], gives an additional support for this proposal. Mn(II) complex **4** spectrum showed two bands at visible region at 435 & 558 nm imputed to $^6A_1 \rightarrow {}^4T_2(G)$ and magnetic moment value 5.25 BM due to metal–metal interactions [41]. For Zn(II) complex **5** as $d^{10}$ system, it has no unpaired electrons, spectra of complex **5** presented two spectral peaks at 455 and 548 nm corresponding to CT (charge transfer) transitions. The observable alterations in ligand peaks are considered as excellent proof for chelate formation [42]. As expected, Zn(II) complex electronic spectrum did not present any valuable information about its stereochemistry and Zn(II) complex exhibited diamagnetic behavior.

### 3.5 ESR Spectral Studies

The electron spin resonance spectrum for $H_2L$-Cu(II), complex **1**, was performed (using powder material at ambient temperature). It provided only value of $g_{eff}$ and doesn't display g perpendicular and g parallel values. The spectrum displayed a broadened feature without hyperfine splitting, because of the dipolar collaboration from the ESR spectrum of a set of magnetic parameters. In Fig. 2, two anisotropic indications were detected in ESR spectrum a of $H_2L$-Cu(II), complex **1**. Profile of ESR spectrum props the suggested geometry of the studied copper complex and harmonize with the results gained from UV/Vis measurement and magnetic studies. The $g_{eff}$ value is 2.1387BM, this observed positive

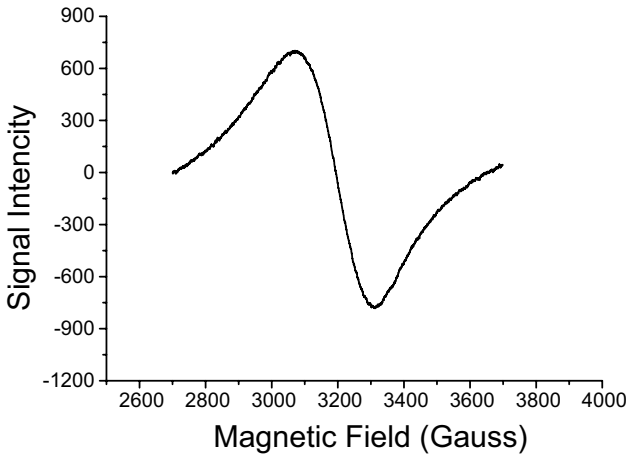


**Fig. 2** ESR spectral band of Cu(II)-complex **1**

deviation from the standard free electron value (2.0023) is attributed to the significant covalent bond interactions among sulfathiazolyl-azo-resorcinol, $H_2L$ and the divalent metal ions under interest. Hence, the metal ions interact with $H_2L$in the inspected complexes in covalent mode, ultimately [43].

On the basis of data obtained from microanalysis, thermal gravimetric analysis, ESR, electronic, IR spectra, subscribing with molar conductance and magnetic moment studies, the bonding of sulfathiazolyl-azo-resorcinol ligand, $H_2L$ to ions and the structure of the investigated complexes **1–5** can be presented as in Fig. 3.

### 3.6 XRD and TEM Inspections

XRD as yet considered one of the best thoughtful approaches, which show advantageous structural microcrystalline data regarding the inspected compounds [44]. Furthermore, it is often used to show an evident view concerning the lattice dynamics of the solid compounds [45]. So, the X-ray diffraction patterns of sulfathiazolyl-azo-resorcinol ligand, $H_2L$and complexes **1–5** were achieved within $0° < 2\theta < 90°$ range of scattering angle. The diffraction patterns of $H_2L$ are perfectly diverse compared with the corresponding metal chelates **1–5** (Fig. 4), up holding complex formation. The sulfathiazolyl-azo-resorcinol ligand patterns displayed good crystallinity while complexes **1–5** were found to be comparatively amorphous. This can be imputed to infrequent configuration for solid frameworks throughout the rapid precipitation process. Overwhelmingly, if the chelation is prompt and/or the product is cooled quickly, the formed compounds will be precipitated compound in an amorphous solid state. Also, some solids are formed in intrinsically amorphous state since their constituents have not the ability to exhibit a good adequate within a crystal lattice. This

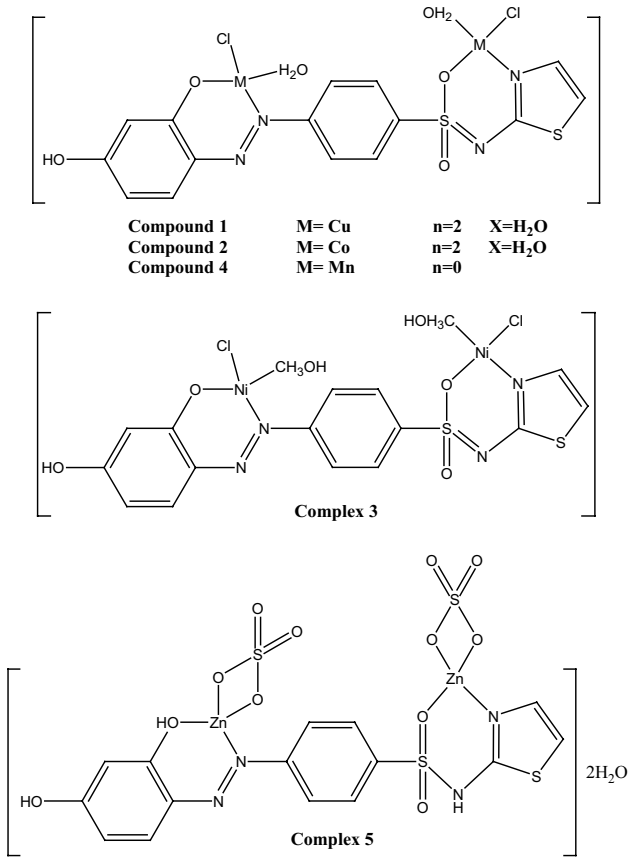


**Fig. 3** Molecular structures of the inspected complexes **1**–**5**

prevents the opportunity for computing d-spacing inside the lattice and/or the crystallite sizes to give a featured insight round the inspected complexes in solid state. The amorphous form reverberates the extremely insignificant size for the groups that is found conveniently in the nano-sized range, which is performed by using transmittance electron microscopy technique [46].

Transmittance electron microscopy (TEM) is usually utilized among the most intrinsic techniques in order to dissect diversified interesting nano-sized metal chelates [47]. It is a largely applied technique for investigation both shape and particle size of solid complexes. High-resolution TEM images were performed for all studied complexes (Fig. 5). We applied TEM here, in order to get evident information relating the surface morphology, particle size, homogeneity, and microstructure for metal complexes (**1**–**5**). The micrographs displayed distinct particle shapes. They showed uniform and homogeneity of surface morphology for all inspected complexes. Moreover, the obtained figures declared the uniformity and propinquity amongst the shapes of particle supporting the existence of congruent matrixes. The spherical feature appearing in images is imputed to the existence of highly symmetric spherical anions in the complexation sphere. Likewise, this may talk place because of the diverse piling up of different singular units of a polycrystalline character. The black zones appeared in the obtained images may be attributed to the combination of extremely small complex molecules. In comparing with the scale bar, the observed particle diameters for all inspected metal complexes were found to be in nano-meter range. The particle sizes reached 59.60 nm for Cu(II) complex **1**, 72.96 nm for Co(II) complex **2**, 83.82 nm for Ni(II) complex **3**, 7.36 nm for Mn(II) complex **4**, and 41.52 nm for Zn complex **5**. These nanometric sizes of the novel synthesized compounds usually enhance the biological efficiency compared with the bulk analogue. This dignified character simplifies the permeability through cell membranes of biological cells. The novel nanosized metal complexes can entice massive concern because of their distinguished functional properties and a magnificent scale of prospective technological uses [48].

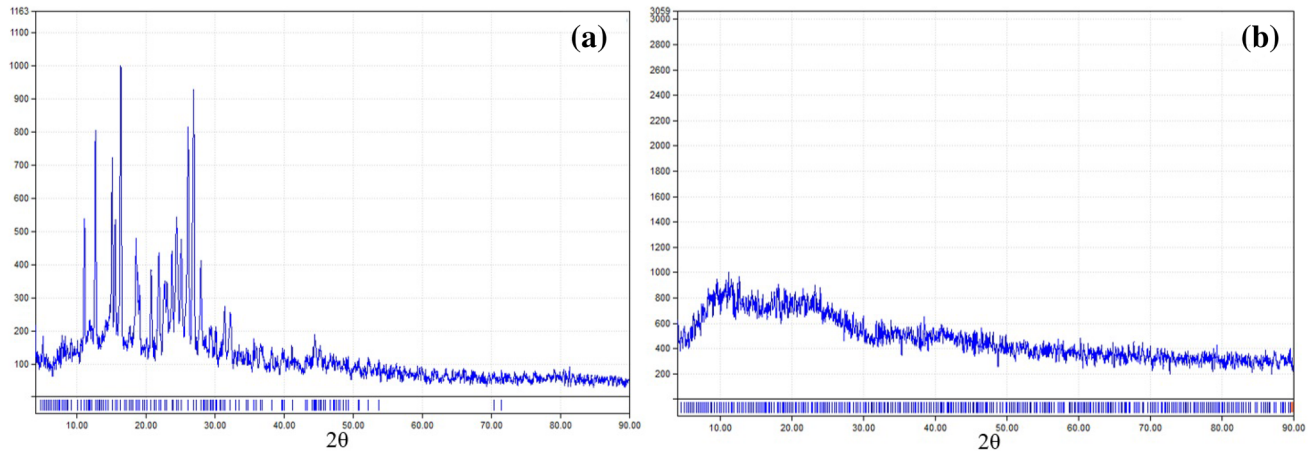


**Fig. 4** X-ray patterns of $H_2L$ (**a**) and Ni(II) complex **3** (**b**)

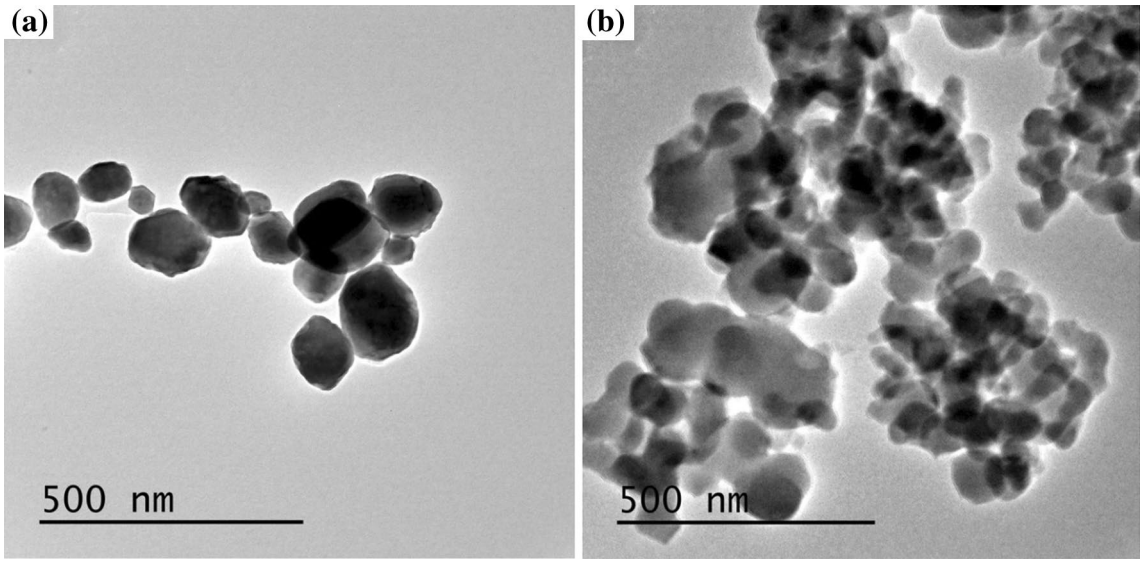


**Fig. 5** Transmission electron micrographs of Cu(II) complex **1** (**a**) and Zn(II) complex **5** (**b**)

## 3.7 Bio-efficiency Studies

### 3.7.1 Evaluation of the Antitumor Activity

Chemotherapy is well known as a main approach for localized and metastasized cancer treatment. Moreover, novel anticancer compounds are indispensable to progress the result for significant magnitude of patients who relapse after extraditing the known and current cancer therapeutic agents [46, 49]. The aim of our study is evaluating the anticancer activities of $H_2L$ and complexes **1**–**5** against human *breast* cancer cell lines (MCF-7 cells) and human *Hepatocellular* carcinoma cell lines (HepG-2 cells). We selected MCF-7 and HepG-2 because they are the most common among other various types of *Carcinomas*. The antitumor activity and growth inhibitory activities were specified by $IC_{50}$ [50]. $IC_{50}$ refers to the concentration of scanned component that decreases cell growth by 50% at the same applied conditions. Every result was computed from the mean of triple measurements and identified as M ± SD. The obtained values for $IC_{50}$ for all investigated compounds are listed in Table 2S. Figure 6 shows the in-vitro antitumor activity of $H_2L$ and its chelates **1**–**5** against HepG-2 cell lines, compared with the applied standard drug cis-DDP. It is trenchant from displayed figures that, most compounds exhibited an inhibition of cell efficacy and the antitumor activity increase distinctly owing to tested compounds against HepG-2 corresponding to the order; Mn(II) complex **4** < $H_2L$ < Zn(II) complex **5** < Ni(II) complex **3** < Co(II) complex **2** < Cu(II) complex (**1**) Among these compounds, Cu(II) complex **1** exhibited the highest activity with $IC_{50}$ = 23.6 µg/ml compared with $IC_{50}$ = 12.23 µg/ml for the slandered drug cis-DDP. This

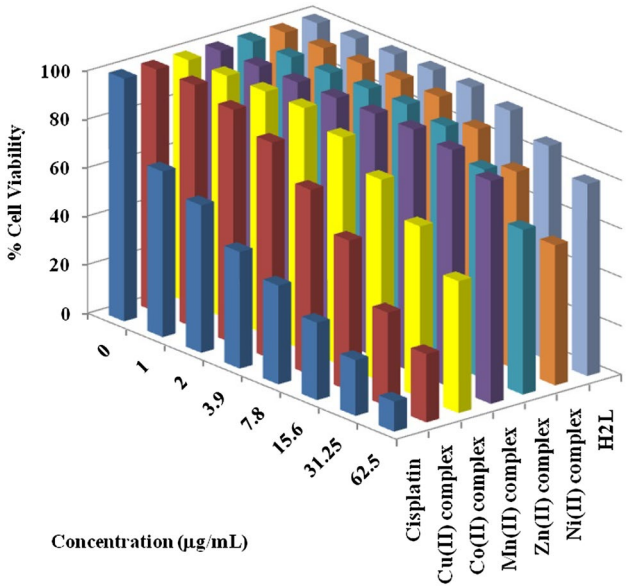


**Fig. 6** The in-vitro antitumor activity of $H_2L$, and its complexes **1**–**5** against HepG-2 cell lines, compared with the applied standard drug cisplatin

compound showed relatively low activity when compared with the previous findings for azo pyrazolone complexes which arrived to $IC_{50}$ = 10.73 µg/ml [51], and arylhydrazonos complexes which reached $IC_{50}$ = 11.80 µg/ml [52], against HepG-2 cells. Figure 7 displays the in-vitro antitumor activity of $H_2L$ and complexes **1–5** towards MCF-7 cell lines, in comparison with 5-flurouracil (the applied standard drug). It is apparent from presented outcomes that, most inspected materials displayed an inhibition of

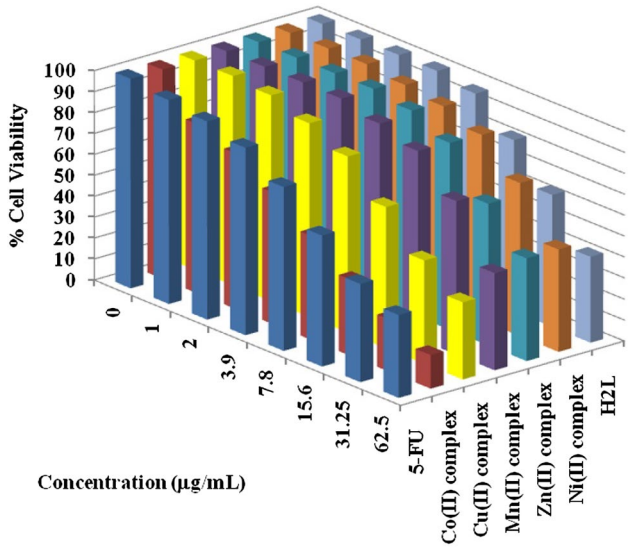


**Fig. 7** The in-vitro antitumor activity of $H_2L$, and its complexes **1**–**5** towards MCF-7 cell lines, in comparison with the applied standard 5-flurouracil

cell viability and increasing the cytotoxic influences related to examined compounds towards MCF-7 according to the order; Ni(II)complex **3** < Zn(II) complex **5** < Mn(II) complex **4** < $H_2L$ < Cu(II) complex **1** < Co(II) complex **(2)** These results represent the great function of both type and properties of metal as well as nature of ligands in limiting the anticancer efficiency of the metal complexes [53, 54]. From these results it is clear that Cu(II) complex **1** showed $IC_{50}$ value = 30.5 µg/ml which is very close to $IC_{50}$ of the applied standard 5-flurouracil with $IC_{50}$ = 28 µg/ml. The promising data is obtained by Co(II) complex **2** showed $IC_{50}$ of 7.67 µg/ml revealing that this compound is much more efficient against MCF-7 cell lines than the applied standard 5-flurouracil. Comparing these results with the literature values reveled that this $IC_{50}$ is greater than the preceding findings for azo pyridine complexes which arrived to $IC_{50}$ = 19.40 µg/ml [55], and azo pyrazolone complexes which arrived to $IC_{50}$ = 12.96 µg/ml [52], against the same cell lines. So, these complexes can be considered quite promising anticancer curing agents which may be applied as new drugs after medicinal studies in the future.

#### 3.7.2 Antibacterial and Antifungal Activities

In-vitro antibacterial and antifungal efficiency of $H_2L$and its chelates **1–5** were screened applying diffusion agar technique [27]. The examined organisms were chosen as follows: *Salmonella typhimurium* (RCMB 006 (1) ATCC 14,028) was selected as example for Gram-negative bacteria and *Staphylococcus aureus* (RCMB010010) was chosen to represent Gram-positive bacteria. Also, we applied *Candida albicans* (RCMB 005003 (1) ATCC 10,231) as a unicellular fungi and *Aspergillus fumigatus* (RCMB 002008) as a higher fungus to represent the multi-cellular fungi. The found data indicated that free ligand is inactive against all tested organisms. Ni(II) complex **3** displayed good activity towards *S. aureus*, within inhibition zone 11.97 mm. Co(II) complex **2** showed high efficiency contra *S. Typhimurium* within 11.13 mm inhibition zone. Such enhanced activity upon complex formation is best clarified on the bases of Overton's concept [56] and Tweedy's chelation theory [57]. The reason of these results may involve hydrogen bond formation between the inspected compounds and the strenuous cell center affecting all cell operations. Likewise, the inspected ligand and its metal chelates perhaps parasitize the respiratory system of the tested organisms and hence restraining the upcoming growth of those organisms. Furthermore, the greater antimicrobial effect of the studied metal chelates is attributable to the turnout of metallic sites. In addition, the cited metal complexes are higher oversensitive against the bacterial cells compared to free ligand (free organic) [58]. The othercompoundswere inactive against the tested organisms. The variation in antimicrobial influence of the metal complexes imputed to the nature of the substituents existing in the chelating agent and nature of metal ions forming the complexes. The above mentioned behavior is owing to the efficacious charge through d-electrons which decreased by electrons donating capacity, whilst it increased due to the electron withdrawing capacity [59].

### 3.8 DNA Binding Studies

#### 3.8.1 Electronic Absorption Spectroscopy Studies

UV/Vis spectroscopy is an essential tool which is applied for evaluating the binding way of DNA with the examined compounds with and the extent of binding as well [28, 60]. The absorption titration experiments were carried out through fixed concentrations of the considered complexes and the free ligand (50 µM) and a successive increasing in DNA concentration at 25 °C from 5 to 45 µM. The absorbance of DNA is cancelled by addition equivalent amounts of DNA to the blank solutions. Absorption spectra for $H_2L$ and its complexes (**1–5**) in the absence and existence of raising concentrations of DNA are presented in Fig. 8. The actual binding constants ($K_b$) of the studied ligand and its chelates with DNA are precisely extracted using the intensity of the CT peaks. In the case of intercalation mode of binding between the compound and DNA, the obvious spectral feature of CT peak is hypochromism with slight shift in wavelength; occasionally no shift is detected. This is because the intercalative type of interaction comprises a significant binding among the aromatic chromophore of the studied chelates and DNA base pairs [61]. The extent of absorbance

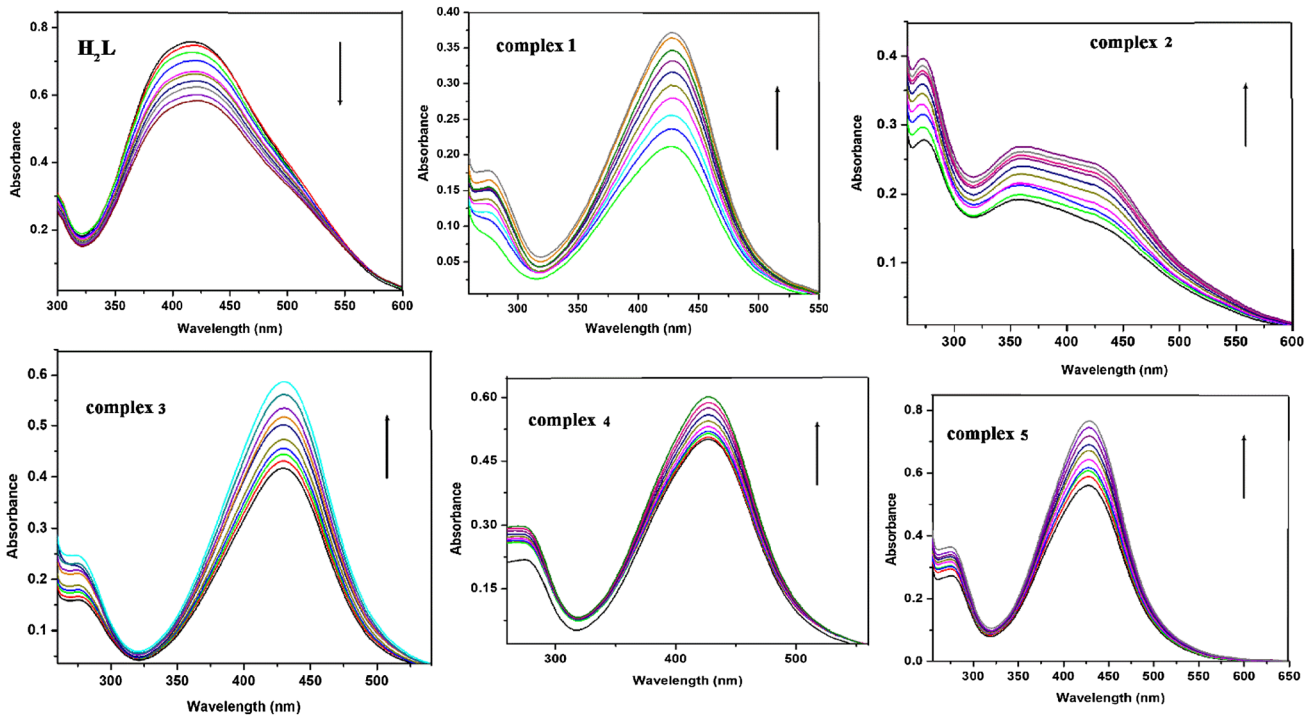


**Fig. 8** Electronic absorption spectra of $H_2L$and its complexes (**1**–**5**) in the absence and existence of rising quantities of SS-DNA

lowering, hypochromism, is ordinarily convenient with the extent of intercalation. The other obvious spectral feature is hyperchromism. The hyperchromism is consistent with the fracturing of the secondary DNA structure [62]. The binding ability and extent of binding between compounds $H_2L$ & complexes **1**–**5** and DNA is discussed based on absorbance as a function of added DNA concentration. The data obtained (Fig. 8) showed by raising the concentration of DNA in the range 5–45 μM, the absorption bands of the $H_2L$ appearing at 414 nm exhibited hypochromism of 23.18% while its complexes (compounds 1–5) underwent hyperchromism of 75.94, 40.5, 40.9, 19.8 and 36.5 for the bands appearing at 428, 360, 431, 427, and 429 nm for compounds **1, 2, 3, 4** and **5**, respectively, suggesting intercalation mode of binding with DNA for $H_2L$ and groove binding for complexes **1**–**5** [28]. To illustrate the quantitative extent of binding of compounds with DNA, $K_b$ is computed by using the following equation:

$$[DNA]/(\varepsilon_a - \varepsilon_f) = [DNA]/(\varepsilon_b - \varepsilon_f) + 1/[K_b(\varepsilon_b - \varepsilon_f)]$$

where [DNA] is the concentration of DNA solution in the base pairs. The absorption coefficients $\varepsilon_a$ equals $A_{obs}$/[compound] while $\varepsilon_f$ and $\varepsilon_b$ refers to the extinction coefficient of the unbounded and the and the compound in a fully bound state to DNA, respectively. The plot of [DNA]/($\varepsilon_a$–$\varepsilon_f$) versus [DNA] is straight line with slope = 1/($\varepsilon_b$–$\varepsilon_f$) and intercept = 1/$K_b$ ($\varepsilon_b$–$\varepsilon_f$); $K_b$ is calculated from the ratio of slope to intercept. The obtained values of the binding constant ($K_b$) were found to be $2.7\times10^4$, $1.04\times10^4$, $6.7\times10^3$, $9.1\times10^3$, $1.8\times10^4$ and $5.2\times10^3$ for $H_2L$, **1, 2, 3, 4**, and **5**, respectively. Analyses of the calculated $K_b$ values of the studied compounds illustrate that the examined compounds have moderate binding ability when these values are compared with ethedium bromide which is the most familiar intercalator [28].

### 3.8.2 Viscosity Measurements

The optical tools provide substantial, but not sufficient, evidence to support the intercalative type of interaction between compounds and DNA. A hydrodynamic tool, like viscosity, that introduces large accuracy to any change in DNA length, is probably the influential tool in order to evaluate the binding mode between tested compounds and DNA. The viscosity of DNA solutions is recorded using different dilutions of the compounds reported in this paper (ligand $H_2L$, and compounds **1**–**5**) using constant concentration of DNA solution. Figure 9 shows the influence of increased quantities of the compounds on DNA viscosity. Viscosity measurement of DNA is regarded a classic way to assess the DNA type of interaction in solution. Under the normal conditions ethidium bromide [EB], as a known example of intercalators, usually results in a considerable enhancement in DNA viscosity which results from the increase in the distance detaching the intercalation sites base pairs that result in a final augmentation in the DNA length [63]. As obvious

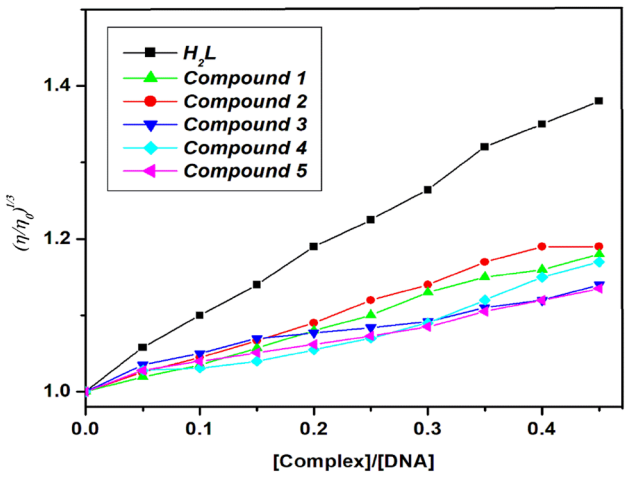


**Fig. 9** Effect of increasing concentrations of $H_2L$ and complexes **1**–**5** on the viscosity of SS-DNA

in Fig. 9, in the case of $H_2L$ there is a raise in the propensity of the viscosity curve by adding increasing amounts of the tested compound which strongly suggests intercalation binding mode between $H_2L$ and DNA resulting from intercalation of the ligand compound among the adjacent DNA base pairs, resulting in elongation in the double spiral and subsequently raising the DNA viscosity, while for the complexes **1**–**5**, the extent of increase in the relative viscosity of DNA solution is slowly over the entire tested range when compared with $H_2L$ suggesting electrostatic force groove binding mode.

## 4 Conclusion

A new azo dye ligand and its homo bi-nuclear divalent Cu, Co, Ni, Mn and Zn complexes were prepared and inspected. Elemental microanalysis, thermal gravimetric analysis (TGA) and molar conductance measurements confirmed formation of non-electrolytic 1:2 (L:M) complexes. The IR spectral studies revealed that the investigated ligand coordinate in a dibasic tetradentate mode *via* N atom of N=N group, uninegative phenolic oxygen, N-atom of thiazole ring and sulfonamide uninegative oxygen. UV–Vis, ESR spectra, magnetic studies and molecular formulae data denoted tetrahedral geometry for all synthesized metal complexes. The XRD patterns revealed the crystalline nature of $H_2L$ and amorphous nature of the complexes. TEM images confirmed the nano-meteric size of all complexes and homogeneous distribution over the complexes surfaces. The antimicrobial screening results proved that the metal chelates were more potent in than the azo dye ligand towards different types of bacteria and fungi. The data obtained for anticancer activity showed that Cu(II) and Co(II) complexes were the most potent anticancer agents. Cu(II) complex **1** exhibited the highest activity with $IC_{50} = 23.6$ µg/ml against HepG-2 cells. Co(II) complex **2** showed the greatest activity with $IC_{50}$ of 7.67 µg/ml revealing that this compound is much more active against MCF-7 cells compared with the applied standard 5-flurouracil, which means that Co(II) complex is a very promising antitumor agent, and attract great interest in further in vivo studies. Both electronic absorption and viscosity measurements confirmed intercalation binding mode between $H_2L$ and SS-DNA while the complexes **1**–**5** interacted with SS-DNA in electrostatic force groove binding mode.

**Acknowledgements** This paper contains the results and findings of a research project that is funded by King Abdulaziz City for Science and Technology (KACST) Grant No. 37–175.

## References

1. J. Feng, S. Zhang, W. Shi, Y. Zhang, Activity of sulfa drugs and their combinations against stationary phase B. burgdorferi in vitro. Antibiotics **6**, 1–11 (2017)
2. D. Das, N. Sahu, S. Mondal, S. Roy, P. Dutta, S. Gupta, T.K. Mondal, C. Sinha, Structures, antimicrobial activity, DNA interaction and molecular docking studies of sulfamethoxazolyl-azo-acetylacetone and its nickel(II) complex. Polyhedron **99**, 77–86 (2015)
3. J.-Y. Winum, A. Maresca, F. Carta, A. Scozzafava, C.T. Supuran, Poly pharmacology of sulfonamides: pazopanib, a multitargeted receptor tyrosine kinase inhibitor in clinical use, potently inhibits several mammalian carbonic anhydrases. Chem. Commun. **48**, 8177–8179 (2012)
4. G. Choquet-Kastylevsky, T. Vial, J. Descotes, Allergic adverse reactions to sulfonamides. Curr. Allergy Asthma Rep. **2**, 16–25 (2002)
5. G.C. Slatore, A.S. Tilles, Sulfonamide hypersensitivity. Immunol. Allergy Clin. N. Am. **24**, 477–490 (2004)
6. M. Summan, A.E. Cribb, Novel non-labile covalent binding of sulfamethoxazole reactive metabolites to cultured human lymphoid cells. Chem. Biol. Interact. **142**, 155–173 (2002)
7. J.H. Al-Fahemi, A.M. Khedr, I. Althagafi, N.M. El-Metwaly, F.A. Saad, H.A. Katouah, Green synthesis approach for novel benzenesulfonamide nanometer complexes with elaborated spectral, theoretical and biological treatments. Appl. Organomet. Chem.32, e4460 (2018)
8. E.M. Mabrouk, K.A. Al-Omary, A.S. Al-Omary, E.H. El-Mossalamy, Electrochemical and spectral studies of some sulfa drug azo dyes and their metal complexes in aqueous solution. J. Adv. Chem. **14**, 6021–6032 (2018)
9. Z.H. Chohan, H.A. Shad, Sulfonamide-derived compounds and their transition metal complexes: synthesis, biological evaluation and X-ray structure of 4 –bromo-2-[(E)-{4-[(3,4-dimethylisoxazol-5 yl)sulfamoyl]phenyl}-iminiomethyl]phenolate. Appl. Organometal. Chem. **25**, 591–600 (2011)
10. M.S. Iqbal, A.H. Khan, B.A. Loothar, I.H. Bukhari, Effect of derivatization of sulfamethoxazole and trimethoprim with copper and zinc on their medicinal value. Med. Chem. Res. **18**, 31–42 (2009)
11. F.A. Saad, J.H. Al-Fahemi, H. El-Ghamry, A.M. Khedr, M.G. Elghalban, N.M. El-Metwaly, Elaborated spectral, modeling, QSAR, docking, thermal, antimicrobial and anticancer activity studies for new nanosized metal ion complexes derived from

sulfamerazineazo dye. J. Ther. Anal.Calori. **131**, 1249–1267 (2018)
12. P. Rani, K.V. Srivastava, A. Kumar, Synthesis and antiinflammatory activity of heterocyclic indole derivatives. Eur. J. Med. Chem. **39**, 449–452 (2004)
13. M. Azam, S.I. Al-Resayes, S.M. Wabaidur, M. Altaf, B. Chaurasia, M. Alam, S.N. Shukla, P. Gaur, N.T.M. Albaqami, M.S. Islam, S. Park, Synthesis, structural characterization and antimicrobial activity of Cu(II) and Fe(III) complexes incorporating azo-azomethine ligand. Molecules **23**, 1–13 (2018)
14. M. Tonelli, I. Vazzana, B. Tasso, V. Boido, F. Sparatore, M. Fermeglia, S.M. Paneni, P. Posocco, S. Pricl, P. Colla, C. Ibba, B. Secci, G. Collu, R. Loddo, Antiviral and cytotoxic activities of aminoarylazo compounds and aryltriazene derivatives. Bioorg. Med. Chem. **17**, 4425–4440 (2009)
15. K.K. Upadhyay, S. Upadhyay, A. Kumar, K. Thapliyal, Synthesis, crystal structures and studies on $Hg^{2+}$ sensing by the diazo derivatives of sulfathiazole and Sulfamethoxazole. J. Sulfur Chem. **33**, 573–582 (2012)
16. G.G. Mohamed, M.A.M. Gad-Elkareem, Synthesis, characterization and thermal studies on metal complexes of new azo compounds derived from sulfa drugs. Spectrochim. Acta A **68**, 1382–1387 (2007)
17. H. Cetisli, M. Karakus, E. Erdem, H. Deligoez, Synthesis, metal complexation and spectroscopic characterization of three new azo compounds. J. Incl. Phen. Macrocycl. Chem. **42**, 187–191 (2002)
18. M.A. Ibrahim, Heterocyclo-substituted sulfa drugs: Part XI. Novel biologically active N-(piperidino-, morpholino-, piperazino-) dithiocarbamyl-azo dyes and their chelates. Phosphorus Sulfur Silicon Relat. Elem. **163**, 219–251 (2000)
19. F.A. Saad, A.M. Khedr, Greener solid state synthesis of nanosized mono and homo bi-nuclear Ni(II), Co(II) Mn(II), Hg(II), Cd(II) and Zn(II) complexes with new sulfa ligand as a potential antitumour and antimicrobial agents. J. Mol. Liq. **231**, 572–579 (2017)
20. H. Li, G.-H. Lee, S.-M. Peng, The first one-dimensional coordination polymer containing O–H···F–Ni hydrogen bonding: crystal structure of $[Ni_3(dpa)_4F_2][Ni_3(dpa)_4(H_2O)_2](BF_4)_2{\cdot}2CH_3OH$. Inorg. Chem. Commun. **6**, 1–4 (2003)
21. R.M. Issa, A.M. Khedr, A. Tawfik, Binuclear mixed metal complexes of V(IV), Mo(III), and U(VI) *o*-cresolphthalein complexonates with other metal ions. Synth. React. Inorg. Met.-Org. Chem. **34**, 1087–1104 (2004)
22. P. Nordell, P. Lincoln, Mechanism of DNA threading intercalation of binuclear Ru complexes: uni- or bimolecular pathways depending on ligand structure and binding density. J. Am. Chem. Soc. **127**, 9670–9671 (2005)
23. A.M. Pyle, J.P. Rehmann, R. Meshoyrer, C.V. Kumar, N.J. Turro, J.K. Barton, Mixed-ligand complexes of ruthenium(II): factors governing binding to DNA. J. Am. Chem. Soc. **111**, 3051–3058 (1989)
24. B. Macías, M.V. Villa, R. Lapresa, G. Alzuet, J. Hernández-Gil, F. Sanz, Mn(II) complexes with sulfonamides as ligands: DNA interaction studies and nuclease activity. J. Inorg. Biochem. **115**, 64–71 (2012)
25. T. Mosmann, Rapid colorimetric assay for cellular growth and survival: application to proliferation and antitumor activity assays. J. Immunol. Methods **65**, 55–63 (1983)
26. S.M. Gomha, S.M. Riyadh, E.A. Mahmmoud, M.M. Elaasser, Synthesis and anticancer activity of arylazothiazoles and 1,3,4-thiadiazoles using chitosan-grafted-poly(4-vinylpyridine) as a novel copolymer basic catalyst. Chem. Heterocycl. Comp. **51**, 1030–1038 (2015)
27. A.C. Scott, Laboratory Control of Antimicrobial therapy. In: J.G et al. eds. Practical Medical Microbiology, 13th edn. (Churchill Livingestone, Edinburgh, 1981)
28. M. Gaber, N.A. El-Wakiel, H. El-Ghamry, S.K. Fathalla, Synthesis, spectroscopic characterization, DNA interaction and biological activities of Mn(II), Co(II), Ni(II) and Cu(II) complexes with [(1H-1,2,4-triazole-3-ylimino)methyl]naphthalene-2-ol. J. Mol. Struct. **1076**, 251–261 (2014)
29. W.J. Geary, The use of conductivity measurements in organic solvents for the characterisation of coordination compounds. Coord. Chem. Rev. **7**, 81–122 (1971)
30. K. Nakamoto, *Infrared spectra of Inorganic and Coordination Compounds* (Wiley, New York, 1986)
31. K.Y. El-Baredie, Preparation and characterization of sulfadiazine schiff base complexes of Co(II), Ni(II), Cu(II), and Mn(II). Monatsh. Chem. **136**, 1139–1155 (2005)
32. K. El-Baradie, R. El-Sharkawy, H. El-Ghamry, K. Sakai, Synthesis and characterization of Cu(II), Co(II) and Ni(II) complexes of a number of sulfa drug azo dyes and their application for wastewater treatment. Spectrochim. Acta A **121**, 180–187 (2014)
33. G.Q. Zhong, J. Shen, Q.Y. Jiang, Y.Q. Jia, M.J. Chen, Z.P. Zhang, Synthesis, characterization and thermal decomposition of $Sb^{III}$-M-$Sb^{III}$ type trinuclear complexes of ethylenediamine-N, N, N′, N′-tetraacetate (M: Co(II), La(III), Nd(III), Dy(III)).J. Therm. Anal. Calorim. **92**, 607–616 (2008)
34. J.R. Allan, W.C. Geddes, C.S. Hindle, A.E. Orr, Thermal analysis studies on pyridine carboxylic acid complexes of zinc(II). Thermochim. Acta C **153**, 249–256 (1989)
35. M. Badea, A. Emandi, D. Marinescu, E. Cristurean, R. Olar, A. Braileanu, P. Budrugeac, E. Segal, Thermal stability of some azo-derivatives and their complexes. J. Therm. Anal. Calorim. **72**, 525–531 (2033)
36. S. Gupta, S. Pal, A.K. Barik, A. Hazra, S. Roy, T.N. Mandal, S.-M. Peng, G.-H. Lee, M.Salah El Fallah, J. Tercero, S.K. Kar, Synthesis, characterization and magnetostructural correlation studies on three binuclear copper complexes of pyrimidine derived Schiff base ligands. Polyhedron **27**, 2519–2528 (2008)
37. P.N. Patel, D.J. Patel, H.S. Patel, Synthesis, spectroscopic, thermal and biological aspects of drug-based copper(II) complexes. Appl. Organomet. Chem. **25**, 454–463 (2011)
38. A.A. Osowole, E.J. Akpan, Synthesis, spectroscopic characterisation, in-vitro anticancer and antimicrobial activities of some metal(ii) complexes of 3-{4, 6-dimethoxy pyrimidinyl) iminomethyl naphthalen-2-ol. Eur. J. Appl. Sci. **4**, 14–20 (2012)
39. M.M. Al-Ne'aimi, M.M. Al-Khuder, Synthesis, characterization and extraction studies of some metal (II) complexes containing (hydrazoneoxime and bis-acylhydrazone) moieties. Spectrochim. Acta A **105**, 365–373 (2013)
40. D.X. West, A. Nassar, F.A. El-Saied, M.I. Ayad, Nickel(II) complexes of 2-aminoacetophenone N(4)-substituted thiosemicarbazones. Transit. Met. Chem. **23**, 423–427 (1998)
41. W. Al Zoubi, A.A.S. Al-Hamdani, S.D. Ahmed, Y.G. Ko, Synthesis, characterization, and biological activity of Schiff bases metal complexes. J. Phys. Org. Chem. **31**, 3752–3759 (2018)
42. D.N. Kumar, B.S. Garg, Synthesis and spectroscopic studies of complexes of zinc(II) with $N_2O_2$ donor groups. Spectrochim. Acta A **64**, 141–147 (2006)
43. T.M.A. Ismail, Mononuclear and binuclear Co(II), Ni(II), Cu(II), Zn(II) and Cd(II) complexes of schiff-base ligands derived from 7-formyl-8-hydroxyquinoline and diaminonaphthalenes. J. Coord. Chem. **58**, 141–151 (2005)
44. A.A. Fahem, Comparative studies of mononuclear Ni(II) and $UO_2$(II) complexes having bifunctional coordinated groups: synthesis, thermal analysis, X-ray diffraction, surface morphology studies and biological evaluation. Spectrochim. Acta A **88**, 10–22 (2012)
45. J.S. Ritch, T. Chivers, K. Ahmad, M. Afzaal, P. O'Brien, Synthesis, structures, and multinuclear NMR spectra of tin(II) and lead(II) complexes of tellurium-containing imidodiphosphinate

ligands: preparation of two morphologies of phase-pure PbTe from a single-source precursor. Inorg. Chem. **49**, 1198–1205 (2010)
46. F.A. Saad, M.G. Elghalban, N. El-Metwaly, H. El-Ghamry, A.M. Khedr, Density functional theory/B3LYP study of nanometric 4-(2,4-dihydroxy-5-formylphen-1-ylazo)-N-(4-methylpyrimidin-2-yl)benzenesulfonamide complexes: quantitative structure–activity relationship, docking, spectral and biological investigations. Appl. Organomet. Chem. **31**, 3721–3735 (2017)
47. J.K. Hui, M.J. MacLachlan, Metal-containing nanofibers via coordination chemistry. Coord. Chem. Rev. **254**, 2363–2390 (2010)
48. A. Salimi, J.R. Halla, S. Soltanian, Immobilization of hemoglobin on electrodeposited cobalt-oxide nanoparticles: direct voltammetry and electrocatalytic activity. Biophys. Chem. **130**, 122–131 (2007)
49. A.S. Sultan, H. Brim, Z.A. Sherif, Co-over expression of Janus kinase 2 and signal transducer and activator of transcription 5a promotes differentiation of mammary cancer cells through reversal of epithelial–mesenchymal transition. Cancer Sci. **2**, 272–279 (2008)
50. S.H. Etaiw, S.A. Amer, M.M. El-Bendary, A Mixed valence copper cyanide $_3$D-supramolecular coordination polymer containing 1,10-phenathorline ligand as a potential antitumor agent, effective catalyst and luminescent material. J. Inorg. Organomet. Polym Mater. **21**, 662–669 (2011)
51. A.F. Shoair, A.A. El-Bindary, N.A. El-Ghamaz, G.N. Rezk, Synthesis, characterization, DNA binding and antitumor activities of Cu(II) complexes. J. Mol. Liq. **269**, 619–638 (2018)
52. E.A. Bakr, G.B. Al-Hefnawy, M.K. Awad, H.H. Abd-Elatty, M.S. Youssef, New Ni (II), Pd (II) and Pt (II) complexes coordinated to azo pyrazolone ligand with a potent anti-tumor activity: synthesis, characterization, DFT and DNA cleavage studies. Appl. Organomet. Chem. 32, e4104 (2018)
53. X. Riera, V. Moreno, C.J. Ciudad, V. Noe, M. Font-Bardía, X. Solans, Complexes of Pd(II) and Pt(II) with 9-aminoacridine: reactions with DNA and study of their antiproliferative activity. Bioinorg. Chem. Appl. 2007, 1–15 (2007)
54. M. Gaber, A.M. Khedr, M. Elsharkawy, Characterization and thermal studies of nano-synthesized Mn(II), Co(II), Ni(II) and Cu(II) complexes with adipohydrazone ligand as new promising antimicrobial and antitumor agents. Appl. Organomet. Chem. **31**, 3885–3898 (2017)
55. W.H. Mahmoud, F.N. Sayed, G.G. Mohamed, Azo dye with nitrogen donor sets of atoms and its metal complexes: synthesis, characterization, DFT, biological, anticancer and Molecular docking studies. Appl. Organomet. Chem. 32, e4347 (2018)
56. A. Kulkarni, S.A. Patil, P.S. Badami, Synthesis, characterization, DNA cleavage and in vitro antimicrobial studies of La(III), Th(IV) and VO(IV) complexes with Schiff bases of coumarin derivatives. Eur. J. Med. Chem. **44**, 2904–2912 (2009)
57. K.N. Thimmaiah, W.D. Lloyd, G.T. Chandrappa, Stereochemistry and fungi toxicity of complexes of p-anisaldehydethiosemicarbazone with Mn(II), Fe(II), Co(II) and Ni(II). Inorg. Chim. Acta **106**, 81–83 (1985)
58. M.A. Phanib, S.D. Dhumwad, Synthesis, characterization and biological studies of $Co^{II}$, $Ni^{II}$, $Cu^{II}$ and $Zn^{II}$ complexes of Schiff bases derived from 4-substituted carbostyrils[quinolin2(1H)-ones]. Trans. Met. Chem. **32**, 1117–1125 (2007)
59. M.I. Abou-Dobara, A.Z. El-Sonbati, M.A. Diab, A.A. El-Bindary, S.M. Morgan, Thermal properties, antimicrobial activity of azo complexes and ultrastructure study of some affected bacteria. J. Microbial. Biochem. Technol. **S3**, 1–13 (2014)
60. T. Hirohama, Y. Kuranuki, E. Ebina, T. Sugizaki, H. Arii, M. Chikira, P.T. Selvi, M. Palaniandavar, Copper(II) complexes of 1,10-phenanthroline-derived ligands: studies on DNA binding properties and nuclease activity. J. Inorg. Biochem. **99**, 1205–1219 (2005)
61. T.R. Li, Z.Y. Yang, B.D. Wang, D.D. Qin, Synthesis, characterization, antioxidant activity and DNA-binding studies of two rare earth(III) complexes with naringenin-2-hydroxy benzoyl hydrazone ligand. Eur. J. Med. Chem. **43**, 1688–1695 (2008)
62. N. Chitrapriya, V. Mahalingam, M. Zeller, K. Natarajan, Synthesis, characterization, crystal structures and DNA binding studies of nickel(II) hydrazone complexes. Inorg. Chim. Acta **363**, 3685–3693 (2010)
63. F.H. Li, G.H. Zhao, H.X. Wu, H. Lin, X.X. Wu, S.R. Zhu, H.K. Lin, Synthesis, characterization and biological activity of lanthanum(III) complexes containing 2-methylene-1,10-phenanthroline units bridged by aliphatic diamines. J. Inorg. Biochem. **100**, 36–43 (2006)